

Magnetic and transport properties of Fe/Cr superlattices (invited)

A. Barthélemy, A. Fert, M. N. Baibich, S. Hadjoudj, and F. Petroff
Laboratoire de Physique des Solides, Université Paris-Sud, 91405 Orsay, France

P. Etienne, R. Cabanel, S. Lequien, F. Nguyen Van Dau, and G. Creuzet
LCR Thomson CSF, 91404 Orsay, France

We describe the magnetic and transport properties of Fe(001)/Cr(001) superlattices grown on GaAs (001) by molecular-beam epitaxy and characterized by reflection high-energy electron diffraction (RHEED), Auger spectroscopy, x-ray diffraction, and electron microscopy. For Cr layers thinner than about 30 Å the magnetic behavior reveals strong antiferromagnetic couplings between the Fe layers across the Cr layers. Polarized neutron diffraction experiments confirm the existence of an antiferromagnetic superstructure. We discuss the origin of the antiferromagnetic (AF) coupling. The Fe/Cr superlattices with AF interlayer coupling exhibit a giant magnetoresistance: when an applied field aligns the magnetizations of the Fe layers, the resistivity drops by a factor of 2 for some samples. This giant magnetoresistance can be ascribed to the spin dependence of the electron scattering by interfaces. We compare our results with the predictions of two recent theoretical models.

I. INTRODUCTION

The ultrathin films, multilayers, and superlattices, which have been extensively studied for several years, present two kinds of interesting properties. First, there are properties associated with the very small thickness of the films or layers, i.e., enhancement or reduction of the magnetic moments, surface or interface anisotropy, low-dimensional effects, etc. In addition, in multilayers and superlattices, there are interesting effects related to the existence of interactions between the layers and to the artificial periodic structure. In rare-earth-based structures, for example, the interlayer magnetic couplings lead to a great variety of magnetic superstructures, such as those found in Gd/Y,¹ Dy/Y,² Dy/Gd,¹ or Er/Y³ superlattices. In the rare earth/yttrium systems the interlayer coupling turns out to be an oscillating function of the yttrium thickness and is due to a RKKY-like exchange interaction between the magnetic layers across the nonmagnetic yttrium layers.⁴

The Fe/Cr system also presents interesting properties associated with antiferromagnetic (AF) interlayer couplings between the Fe layers across Cr layers. The existence of such AF coupling has first been found in Fe/Cr/Fe sandwiches in the light scattering experiments of Grünberg *et al.*⁵ and the spin-polarized low-energy electron diffraction (SPLEED) measurements of Carbone and Alvarado.⁶ In this paper we review experimental data on Fe(001)/Cr(001) superlattices grown by molecular-beam epitaxy (MBE).

We describe the preparation and characterization of the Fe(001)/Cr(001) superlattices in Sec. II and the results of magnetization, and neutron diffraction experiments⁷⁻⁹ in Sec. III. AF interlayer couplings appear for Cr layers thinner than about 20 Å. In the magnetization and torque measurements, the signature of the AF couplings is a tilt of the magnetization loops and a change of sign in the torque ver-

sus field curves. In the neutron diffraction experiments, the observation of a small-angle Bragg peak at the wave vector corresponding with twice the chemical period of the superlattice confirms the existence of an AF superstructure.¹⁰ By analyzing the magnetization curves we can derive the coupling constant as a function of the chromium thickness. The interlayer coupling is always AF, increases as the Cr thickness decreases (down to 9 Å), and subsists well above the Néel temperature of chromium. It can be ascribed to exchange interactions between the Fe moments across Cr. The interpretation of this interlayer exchange interaction raises interesting problems, as discussed in Sec. II C and also in Ref. 11.

An additional and outstanding interest of the Fe/Cr superlattices is the giant magnetoresistance that we observe for antiferromagnetically coupled systems.^{9,12} The magnetoresistance data are presented in Sec. IV. The resistivity drops when an applied field overcomes the AF coupling and aligns the magnetic moments of the Fe layers. The resistivity change is surprisingly large: $\rho/\rho(H=0) \approx 1/2$ for samples with the thinnest Cr layers (9 Å) (this turns out to be very promising for applications to magnetoresistive sensors). We have ascribed the large magnetoresistance of the Fe/Cr superlattices to spin-dependent interface scattering,^{9,11} an effect related to the spin-dependent impurity scattering observed in bulk ferromagnetic transition metals.¹³ In Sec. IV B, we describe this interpretation and we discuss recent theoretical models.^{11,14} Note that a relatively large (a few percent) magnetoresistance, probably due to a similar mechanism, has also been observed in Fe/Cr/Fe¹⁵ and Co/Au/Co^{16,17} sandwiches.

II. GROWTH AND CHARACTERIZATION

The growth of our Fe(001)/Cr(001) superlattices and their characterization have been presented elsewhere and are

also described in Ref. 18. The superlattices have been grown by MBE on GaAs (001) substrates and characterized by reflection high-energy electron diffraction (RHEED), Auger electron spectroscopy (AES), x-ray diffraction, and scanning transmission electron microscopy (STEM). The data from the AES profile and STEM cross section rule out any significant intermixing of Fe and Cr. However, these AES and STEM techniques cannot provide us with quantitative data on the interface roughness *at the atomic scale*.

Since the beginning of 1988 we have prepared several series of superlattices, with Cr and Fe thicknesses (t_{Cr} and t_{Fe}) ranging from 9 to 90 Å. The conditions of growth have progressively improved. The last series have been prepared with the substrate temperature (70–100 °C) and the deposition rate (0.2 Å/s) which appear to give the highest values to the antiferromagnetic coupling and to the magnetoresistance.

III. MAGNETIC PROPERTIES

The most interesting properties—those arising from magnetic coupling between the Fe layers through Cr—appear in our experiments for Cr layers thinner than about 20 Å. Before describing these properties we first summarize data obtained for uncoupled superlattices and previously reported.^{7,8} For the superlattices with $t_{Cr} \geq 30$ Å the magnetic behavior is determined by the magnetocrystalline and shape anisotropies. The magnetization is always in the plane of the layers (the interface anisotropy—derived from torque measurements—is too weak to overcome the shape anisotropy, even for the samples with the thinnest Fe layers). In the layer plane the easy axes are [100] and [010] with, from torque data, $K_1 \approx 52 \times 10^4$ erg/cm³ for the anisotropy constant (usual notation). The coercive fields range between 50 and 100 Oe. The saturation magnetizations per volume unit of iron M_s are scattered between 1300 and 1700 emu/cm³ (the small deficit with respect to the 1700 emu/cm³ of bulk iron might be due to a small negative contribution from the chromium layers).

A. Magnetization curves for Fe/Cr superlattices with interlayer coupling

Figure 1 shows magnetization curves for samples with different Cr thicknesses in applied fields along [110] in the layer plane. As the Cr thickness decreases from 60 to 9 Å it becomes harder and harder to saturate the magnetization—the curves are more and more tilted—and the remanent magnetization decreases to a very small value. This is what is expected for Fe layers antiferromagnetically coupled through Cr. In a simple model assuming a fixed magnetic moment for each Fe layer ($M_s t_{Fe}$ per surface unit) and an AF coupling between neighbor Fe layers of the form $\hat{J}\hat{M}_1 \cdot \hat{M}_2$ (J is the coupling constant per surface unit), one expects a linear variation of the magnetization with the applied field H (Ref. 7):

$$M = M_s^2 t_{Fe} H / 4J \quad (1)$$

and a saturation field

$$H_S = 4J / M_s t_{Fe}. \quad (2)$$

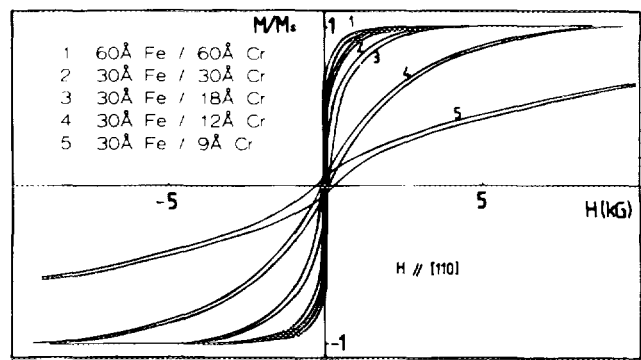


FIG. 1. Magnetization curves at 4.2 K with an applied field along [110] in the layer plane for several Fe(001)/Cr(001) superlattices. The saturation magnetizations M_s are between 1300 and 1700 emu/cm³. The measurements presented in this figure have been obtained with a vibrating sample magnetometer and the contribution from the GaAs substrate has been subtracted. Magnetization curves obtained with a SQUID magnetometer have been presented in Ref. 9.

The progressive tilt of the experimental curves is thus ascribed to a progressive increase of J . Such an oversimplified model can be improved by introducing the magnetic anisotropy^{8,19} and also by taking into account the finite magnetic stiffness of the Fe layers.⁸ With an anisotropy energy per surface unit $K_1 t_{Fe} \sin^2 2\phi/4$ (ϕ is the angle of M with [100]) and for small enough values of K_1/J , one finds a nonlinear field dependence of M and different saturation fields in the easy and hard direction of the layer plane:

$$\begin{aligned} H_S^{[100]} &= \frac{4J}{M_s t_{Fe}} - \frac{2K_1}{M_s}, \\ H_S^{[110]} &= \frac{4J}{M_s t_{Fe}} + \frac{2K_1}{M_s}. \end{aligned} \quad (3)$$

For most of our samples, the correction to H_S arising from K_1 is relatively small. This can be seen from the small difference we observe between $H_S^{[100]}$ and $H_S^{[110]}$, and is also in agreement with the value of K_1 derived from torque measurements (the above quoted value of K_1 corresponds to $2K_1/M_s \approx 0.6$ kG to be compared with experimental values of H_S larger by an order of magnitude or more). Taking into account the finite magnetic stiffness and the different orientation of the magnetization at the center and the edges of the Fe layers also modifies the magnetization curves and enhances H_S with respect to Eqs. (1)–(3)⁸ but not significantly. Consequently, for our samples, Eq. (1) is a convenient approximation and $H_S t_{Fe} / 4M_s$ is a simple and direct estimate of the coupling constant (a more detailed analysis, taking into account the anisotropy and the finite stiffness, will be published elsewhere).

Figure 2 presents our experimental values of the saturation field H_S for superlattices with $t_{Fe} = 30$ Å together with the normalized saturation field, i.e., $H'_S = H_S t_{Fe} / 30$, for a few superlattices with $t_{Fe} \neq 30$ Å (in fact these values of H_S are derived from the magnetoresistance curves for which the saturation field is more accurately defined). The main features of the experimental data of Fig. 2 are a *continuous increase of the coupling constant as t_{Cr} decreases from 18 to 9 Å*. There is some scattering of the data on both sides of the

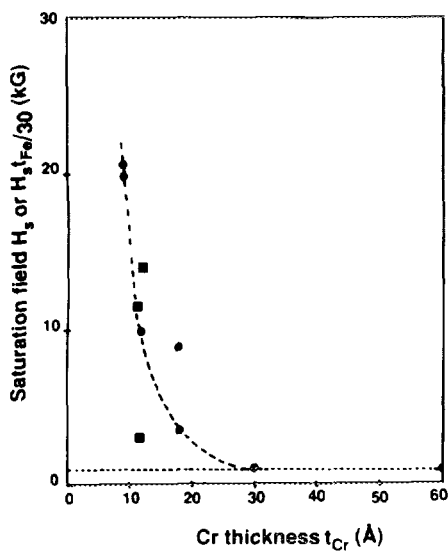


FIG. 2. Dependence of the AF interlayer coupling on the Cr thickness t_{Cr} . Circles: saturation field vs t_{Cr} for superlattices with $t_{Fe} = 30 \text{ \AA}$. Squares: normalized saturation field $H_s^1 = H_s \times t_{Fe} / 30$ (with t_{Fe} in \AA) vs t_{Cr} for superlattices with t_{Fe} different from 30 \AA ($t_{Fe} = 12$ or 16 \AA). $H_s = 20.6 \text{ kG}$ (with $t_{Fe} = 30 \text{ \AA}$) corresponds with $J = 1.38 \text{ meV}$ per unit cell of the interface ($2.8 \times 2.8 \text{ \AA}^2$) for the coupling constant. The dashed line is to guide the eye. The saturation fields are those derived from magnetoresistance curves with H along $[110]$. The values derived from magnetization curves are nearly the same (but less accurately defined).

dashed line we have drawn to guide the eye in Fig. 2. We suppose this scattering arises from the dependence of the interlayer coupling on the quality of the interfaces. We have investigated the influence of the growth conditions on the interlayer coupling. The conditions that give the highest values of H_s (and also the highest magnetoresistance) are quoted in Sec. II.

The absolute values of the coupling constant J calculated from H_s are surprisingly large. Taking the superlattice (Fe 30 \AA /Cr 9 \AA)₄₀ as an example, we find $H_s = 20.6 \text{ kG}$ and we derive from Eq. (1) that the value of J per unit cell of the interface ($2.8 \times 2.8 \text{ \AA}^2$) amounts to 1.38 meV [by comparison, in bulk iron, when the coupling between two neighbor (001) Fe plans is written as $-J_0 \mathbf{M}_1 \cdot \mathbf{M}_2$, the value of J_0 is about 100 meV per unit cell²⁰].

A typical example of the temperature dependence of the saturation field H_s is shown in Fig. 3. H_s decreases by only 14% between 4.2 and 350 K. As, in the same temperature range, the saturation magnetization M_s decreases by about 9%, we derive from Eq. (1) that the coupling constant J decreases by about 23%. This means that the AF coupling is not very temperature dependent and is still very strong at 350 K, well above the Néel temperature of bulk chromium ($T_N \approx 310 \text{ K}$). This is an important result as it demonstrates that the interpretation of the AF interlayer coupling cannot be based on the antiferromagnetism of bulk chromium.

B. Neutron diffraction

Preliminary measurements have been carried out on a three-axis polarized spectrometer IN20 at the Institut Laue Langevin (Grenoble). Since the c axis is perpendicular to

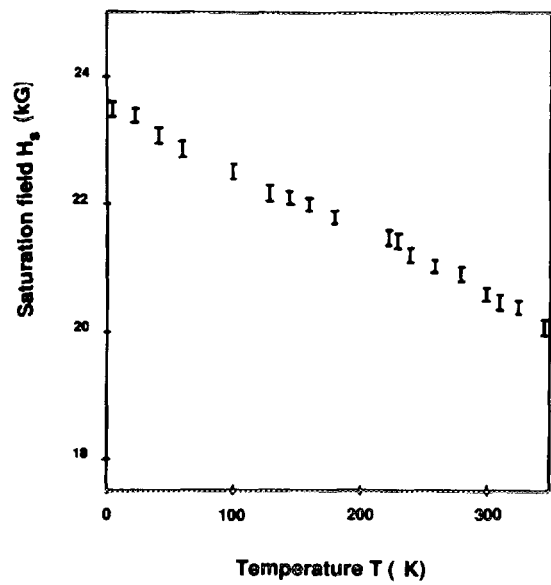


FIG. 3. Temperature dependence of the saturation field H_s for a (Fe 16 \AA /Cr 12 \AA)₂₀ superlattice.

the multilayer surface and colinear to the modulated magnetic structure, the experiments have been performed in the reflection geometry at only low q values. With polarization analysis, one can investigate the spin direction with respect to the vertical applied field H (i.e., in the film plane) used to maintain the neutron polarization and to magnetize the sample. Magnetic scattering is non-spin-flip if the spins are aligned along H and is spin-flip if the spins are perpendicular to H . In Fig. 4 is reported raw spin-flip intensity versus q for the AF peak of a Fe/Cr superlattice ($D_{SL} = 45 \text{ \AA}$). Details will be published elsewhere.²¹ We started the experiment at $H = 1 \text{ kG}$ where a single AF domain is achieved. The AF peak position ($q = 0.084 \text{ \AA}^{-1}$) is slightly above that expected from the nuclear peak position ($q = 0.14 \text{ \AA}^{-1}$), which is due to refraction and reflection effects. The intensity decreases rapidly when H increases. We find that all the spins of the Fe layers are aligned along the applied field for $H = 8 \text{ kG}$ that saturates the magnetization at 1.6 K .

C. Interlayer coupling—discussion

We first summarize the main features of the interlayer coupling found in the Fe(001)/Cr(001) superlattices:

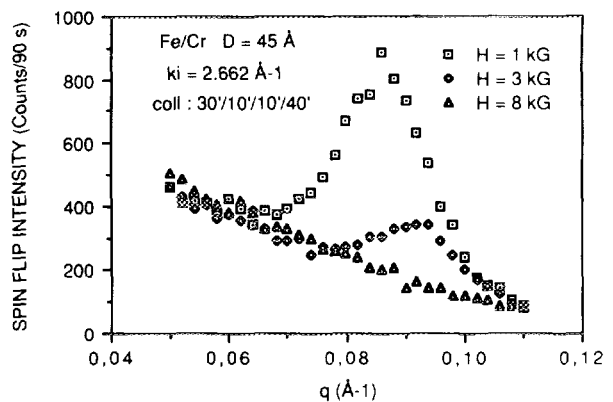


FIG. 4. Field dependence of the spin-flip intensity vs q for a (Fe 30 \AA /Cr 15 \AA)₂₀ superlattice at 1.6 K .

(i) An AF interlayer coupling appears for $t_{Cr} < 20 \text{ \AA}$ and, although there is some scattering of the data in Fig. 2, its strength seems to increase continuously when t_{Cr} decreases.

(ii) The AF coupling decreases slightly as the temperature increases and is still strong well above the Néel temperature of bulk Cr, $T_N \approx 310 \text{ K}$.

(iii) The coupling constant J reaches 1.38 meV per unit cell of the interface ($2.8 \times 2.8 \text{ \AA}^2$) for the thinnest Cr layers (9 \AA). Puzzlingly, the AF coupling in Fe/Cr/Fe sandwiches seems to be smaller.⁵

The AF interlayer coupling of the Fe/Cr superlattices is much too strong to be due to dipole interactions²² and must be ascribed to exchange coupling through the Cr layers.

Let us suppose first that the Cr layer retains the spin density wave (SDW) structure of bulk Cr, with a wavelength close to the lattice parameter. As this is described by Hinchey and Mills²³ for F/AF multilayers, this would give an interlayer coupling oscillating as a function of t_{Cr} . This oscillation is not observed. Moreover, the interlayer coupling is still strong well above the Néel temperature of Cr. This rules out this type of approach. Probably the electronic structure of Cr is strongly affected by the proximity of Fe and does not present the SDW structure of Cr.

An alternative approach consists in ascribing the interlayer coupling to a RKKY-like interaction, either based on free electrons to carry the interaction, or taking into account the tendency of Cr to develop SDW (as in the Yafet model for Y/Gd superlattices.⁴) In both cases, the resulting interlayer interaction is expected to oscillate as a function of t_{Cr} , again in discrepancy with our experimental data.

As such simple perturbation models do not fit with experiments, we have tried a nonperturbative approach, that is, an *ab initio* calculation of the band structure of Fe(001)/Cr(001) supercrystals. These calculations, which find a lower ground-state energy for antiparallel magnetizations in neighbor Fe layers, are presented in Ref. 11.

IV. GIANT MAGNETORESISTANCE

A. Experimental results

We have measured the resistivity and magnetoresistance of Fe/Cr superlattices with a conventional ac method. A typical value of the resistivity at 4.2 K is $60 \mu\Omega \text{ cm}$ for a bilayer thickness around 30 \AA .

Figures 5 and 6 present magnetoresistance curves of Fe/Cr superlattices at 4.2 K with magnetic field and current along a $[110]$ direction in the plane of the multilayer. We find a large negative magnetoresistance for the samples exhibiting AF interlayer coupling (and a vanishingly small effect in samples without AF coupling). The resistivity drops during the magnetization process and becomes practically constant when the magnetic moments of the Fe layers have been aligned, i.e., for $H > H_S$. For an applied field perpendicular to the current in the layer plane or perpendicular to the layers the resistivity drop is nearly the same (the very small difference comes from the contribution of the conventional resistivity anisotropy which is less than 1%). The main result is the huge value of the magnetoresistance: for the (Fe 30 \AA /Cr 9 \AA) superlattice in Fig. 5 there is almost a factor of

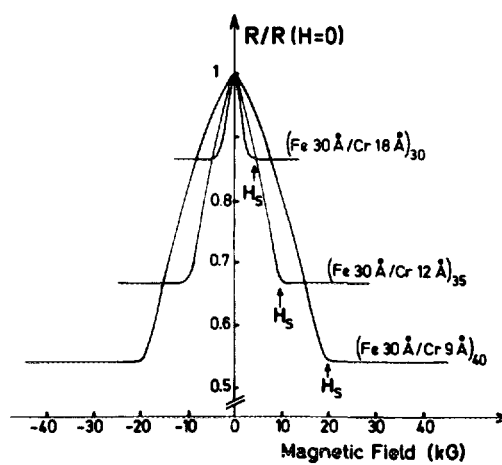


FIG. 5. Magnetoresistance of three Fe/Cr superlattices with the same Fe thickness and different Cr thicknesses. The current and the applied field are along $[110]$ in the plane of the layers. There is a small difference between the curves in increasing and decreasing fields (hysteresis) that we have not represented on the figure.

2 between the resistivities at zero field and at $H > H_S$. The magnetoresistance found in Fe/Cr/Fe sandwiches exhibits a similar behavior but is definitely smaller.¹⁵

The magnetoresistance steeply decreases as t_{Cr} increases. This clearly shows up in Fig. 5 which presents data on samples with the same value of t_{Fe} and different values of t_{Cr} . The magnetoresistance also decreases—but less significantly—when t_{Fe} increases. This appears in Fig. 6 which presents data on samples with $t_{Cr} = 12 \text{ \AA}$ and different values of t_{Fe} .

Figure 7 shows the temperature dependence of the magnetoresistance. In comparison with 4.2 K , the reduction factor at room temperature is about 0.4 for almost all our samples. Nevertheless the magnetoresistance is still very high at room temperature.

Finally we mention that the magnetoresistance is very sensitive to thermal treatments. We have found that annealing our samples at $215 \text{ }^\circ\text{C}$ during 1 h strongly reduces the magnetoresistance (without affecting significantly the mag-

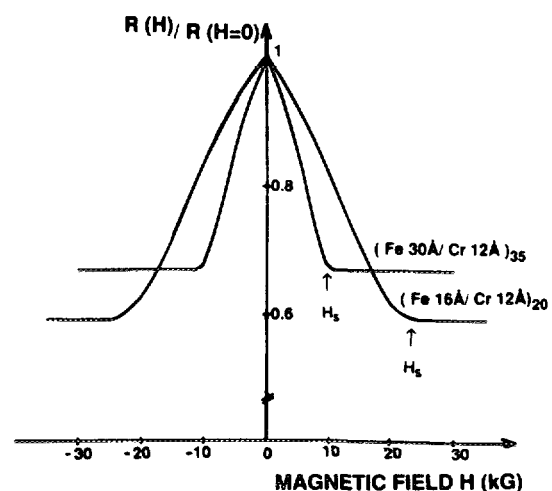


FIG. 6. Same caption as Fig. 5 but for superlattices with the same Cr thickness and different Fe thicknesses.

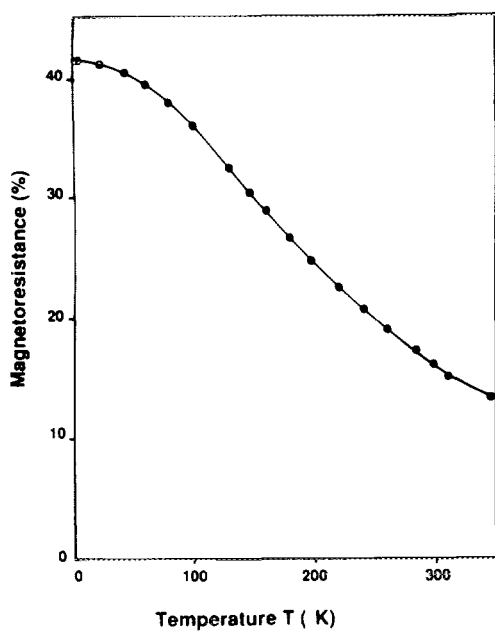


FIG. 7. Temperature dependence of the magnetoresistance. $[R(H=0) - R(H > H_S)]/R(H=0)$ is plotted vs T for a (Fe 16 Å/Cr 12 Å)₂₀ superlattice.

netic behavior and H_S). Also the magnetoresistance is dependent on the growth conditions. We have quoted in Sec. II the growth parameters used to obtain the optimal magnetoresistance. As will be discussed below, this dependence on the growth and annealing parameters is probably due to the crucial role of the interface roughness for the transport properties of multilayers. Up to now our characterizations of the roughness (by AES and STEM) have not been sensitive enough to correlate quantitatively magnetoresistance and interface roughness.

B. Discussion

We have ascribed the giant magnetoresistance of the Fe/Cr superlattices to spin-dependent interface scattering.¹² Theoretical models based on this mechanism have been worked out by Camley and Barnas¹⁴ and by Levy and co-workers.^{11,24} Recently a model based on spin-dependent tunneling has also been proposed.²⁵

Spin-dependent interface scattering is related to the spin-dependent impurity scattering observed in ferromagnetic metals such as Ni, Fe, or Co.¹³ In these metals, the electron current is carried mainly by the s band electrons and, at $T \ll T_c$, without spin-flip scattering (because the main spin-flip scattering mechanism is via exchange interaction with the d electrons, that is, through creation or annihilation of spin waves). Consequently the current is carried by the spin \uparrow and spin \downarrow electrons²⁶ in two independent channels. This is the "two-current model."¹³ The two currents can be very different because certain transition metal impurities scatter the spin \uparrow and spin \downarrow electrons very differently. This is due to combined effects involving the spin splitting of the host d band, the spin splitting of the impurity d levels and the different hybridization between the host and impurity d states for the spin \uparrow and spin \downarrow directions.²⁷ For example, Cr impuri-

ties in Fe scatter much more strongly the spin \uparrow electrons, which results in a ratio of 6 between the resistivities of the spin \uparrow and spin \downarrow channels, $r = \rho_{\uparrow}/\rho_{\downarrow} \approx 6$.¹³ The total current is carried by the spin \uparrow and spin \downarrow channels in parallel, so that the low-temperature impurity resistivity is written as

$$\rho_0 = \rho_{\uparrow}\rho_{\downarrow}/(\rho_{\uparrow} + \rho_{\downarrow}).$$

With $\rho_{\downarrow} \ll \rho_{\uparrow}$ one gets $\rho_0 \approx \rho_{\downarrow}$, which expresses the short-circuit effect by the less scattered electrons.

At high temperatures, the spin-flip scattering by collision with spin waves becomes significant. When the spin-flip rate exceeds the impurity scattering rates— $\rho_{\uparrow\downarrow} \gg \rho_{\uparrow}, \rho_{\downarrow}$ in the conventional notation—the spin \uparrow and spin \downarrow current are "mixed" and the impurity resistivity becomes an average of ρ_{\uparrow} and ρ_{\downarrow} :

$$\rho_1 = (\rho_{\uparrow} + \rho_{\downarrow})/4.$$

When ρ_{\uparrow} and ρ_{\downarrow} are very different, ρ_1 is much larger than ρ_0 [$\rho_1/\rho_0 = (1+r)^2/4r$]. Such an enhancement of the impurity contribution to the resistivity by "spin mixing" has been observed in many Ni-, Fe-, or Co-based alloys.¹³

The magnetoresistance of the Fe/Cr superlattices can be accounted for by an effect of "spin mixing" by alternating magnetizations similar to the spin mixing by spin waves that enhances the impurity resistivity in bulk metals. The basic assumption is that there exists spin-dependent scattering. For example, if we imagine that the scattering by interface roughness is equivalent of the scattering by Cr(Fe) impurities in Fe(Cr), we expect a significant spin dependence.

To describe more precisely the mechanism of the magnetoresistance we have first to consider the simplest case: (i) electron mean free path λ much larger than the layer thickness, (ii) non-spin-flip scattering, that is, $T \ll T_c$. For $H > H_S$ the magnetizations of all the Fe layers are parallel, there is a spin direction that is less scattered at *all the interfaces* and the resulting short-circuit effect leads to the resistivity $\rho_0 = \rho_{\uparrow}\rho_{\downarrow}/(\rho_{\uparrow} + \rho_{\downarrow})$ where ρ_{\uparrow} and ρ_{\downarrow} are the resistivities in the spin \uparrow and spin \downarrow channels. In contrast, for $H = 0$, an electron with a given spin is alternately weakly and strongly scattered, which leads to an average value of the resistivity, $\rho_1 = (\rho_{\uparrow} + \rho_{\downarrow})/4$. The resistivity drop from ρ_1 to ρ_0 during the magnetization of the sample can be large if ρ_{\uparrow} and ρ_{\downarrow} are very different.

Now suppose that t_{Cr} increases and becomes larger than the mean free path λ . From the general properties of the Boltzmann equation, the perturbation of the electron distribution function cannot extend farther than λ . For $t_{Cr} \gg \lambda$, there will be an electron layer of thickness λ around each interface affected by the scattering at this interface but completely independent of the magnetization at the other interfaces. The magnetoresistance will vanish as $\exp(-t_{Cr}/\lambda^*)$ (with λ^* of the order of magnitude of λ).

The magnetoresistance is also expected to decrease as the temperature increases. This is first because the collisions with spin waves will tend to equalize the spin \uparrow and spin \downarrow currents, secondly because the reduction of λ enhances t_{Cr}/λ .

The mechanism qualitatively described above and the corresponding theoretical models^{11,14,24} explain the main features of the experimental results. The ratio $\rho_{\uparrow}/\rho_{\downarrow} \approx 6$

found for Cr impurities in bulk Fe¹³ can account for the large value of the magnetoresistance. The reduction of the magnetoresistance at room temperature can be mainly ascribed to the onset of spin-flip scattering (the temperature dependence of λ is too small for a significant effect). The strong reduction of the magnetoresistance as t_{Cr} increases (Fig. 7) is consistent with a variation as $\exp(-t_{Cr}/\lambda^*)$. However, the small number of experimental data does not allow us a reliable test of the predicted thickness dependence. Moreover, there are discrepancies between the values of the magnetoresistance found in different groups that are hard to understand.

Finally we point out that the spin dependence could also be attributed to the scattering within the Fe layers (Cr impurities for example) and not to the scattering by the interface roughness. With such an assumption the magnetoresistance is expected to collapse as $\exp[-(t_{Fe} + 2t_{Cr})/\lambda^*]$. The experimental data seem in better agreement with the variation as $\exp(-t_{Cr}/\lambda^*)$ expected from spin-dependent interface scattering but a spin dependence of the scattering within the Fe layers cannot be ruled out completely.

V. CONCLUSIONS

The Fe/Cr superlattices exhibit interesting properties, which are far from being completely understood. Magnetization and neutron measurements show that the Fe layers are antiferromagnetically coupled across the Cr layers for Cr thickness between 9 Å—our thinnest layers—and 20 Å. We find that the AF interlayer coupling steeply increases as t_{Cr} decreases and is weakly temperature dependent up to 350 K. We ascribe it to exchangelike interactions through Cr. However, the AF coupling cannot be accounted for by SDW effects in Cr or a RKKY-like mechanism. Band-structure calculations of Fe/Cr supercrystals show that the Cr layers are strongly perturbed by the proximity of Fe and suggest the AF coupling arises from spin-dependent hybridization effects.¹¹

A huge variation of the resistivity is observed during the magnetization process of the AF coupled Fe/Cr superlattices. We ascribe this giant magnetoresistance to the spin dependence of the electron scattering at the Fe/Cr interfaces. More experimental results, especially extensive data on the thickness dependence of the magnetoresistance, are needed for a better test of the theoretical models. As spin-dependent scattering is observed in many Fe, Ni, and Co alloys, it should also be possible to study similar magnetoresistance effects in other multilayered systems.

Note added in proof: Interesting new results on Fe/Cr are reported in these proceedings [see: J. J. Krebs, P. Lubitz, A. Chaiken, and G. A. Prinz; A. Chaiken, G. A. Prinz, and J. J. Krebs; S. S. P. Parkin, S. Fan, N. More, and K. P. Roche;

and also J. J. Krebs, P. Lubitz, A. Chaiken, and G. A. Prinz, *Phys. Rev. Lett.* **63**, 1645 (1989)].

- ¹ C. F. Majkrzak, D. Gibbs, P. Böni, A. I. Goldman, J. Kwo, M. Hong, T. C. Hsieh, R. M. Fleming, D. B. Mc Whan, Y. Yafet, J. W. Cable, J. Bohr, H. Grimm, and C. L. Chien, *J. Appl. Phys.* **63**, 3447 (1988).
- ² R. W. Erwin, J. J. Rhyne, M. B. Salamon, J. Borchers, S. Sinha, J. E. Cunningham, and C. P. Flynn, *Phys. Rev. B* **35**, 6808 (1987).
- ³ J. A. Borchers, G. Nieuwenhuys, M. B. Salamon, C. P. Flynn, R. Du, and W. Erwin, *J. Phys. (Paris) Colloq.* **49**, C8-1685 (1989).
- ⁴ Y. Yafet, *J. Appl. Phys.* **61**, 4058 (1987).
- ⁵ P. Grünberg, R. Schreiber, Y. Pang, M. B. Brodsky, and H. Sowers, *Phys. Rev. Lett.* **57**, 2442 (1986).
- ⁶ C. Carbone and S. F. Alvarado, *Phys. Rev. B* **36**, 2433 (1987).
- ⁷ F. Nguyen Van Dau, A. Fert, P. Etienne, M. N. Baibich, J. M. Broto, G. Creuzet, A. Friederich, S. Hadjoudj, H. Hurdequint, and J. Massies, *J. Phys. (Paris) Colloq.* **49**, C8-1633 (1988).
- ⁸ F. Nguyen Van Dau, thesis, Orsay 1989.
- ⁹ A. Barthelemy, M. N. Baibich, J. M. Broto, R. Cabanel, G. Creuzet, P. Etienne, A. Fert, A. Friederich, S. Lequien, F. Nguyen Van Dau, and K. Ounadjela, in *Growth, Characterization, and Properties of Ultrathin Magnetic Films and Multilayers*, edited by B. T. Jonker, E. E. Marinero, J. P. Heremans, MRS Proceedings Vol. 151 (MRS, Pittsburgh, PA, 1989), p. 43.
- ¹⁰ S. Lequien, C. Vettier, and M. Hennion (to be published).
- ¹¹ P. M. Levy, K. Ounadjela, C. B. Sommers, A. Fert and S. Zhang (these proceedings).
- ¹² M. W. Baibich, J. M. Broto, A. Fert, F. Nguyen Van Dau, F. Petroff, P. Etienne, G. Creuzet, A. Friederich, and J. Chazelas, *Phys. Rev. Lett.* **61**, 2472 (1988).
- ¹³ A. Fert and I. A. Campbell, *J. Phys. F* **6**, 849 (1976); I. A. Campbell and A. Fert, *Ferromagnetic Materials*, edited by E. P. Wohlforth (North-Holland, Amsterdam, 1982), p. 769.
- ¹⁴ R. E. Camley and J. Barnas, *Phys. Rev. Lett.* **63**, 664 (1989).
- ¹⁵ G. Binash, P. Grünberg, F. Saurenbach, and W. Zinn, *Phys. Rev. B* **39**, 4828 (1989).
- ¹⁶ E. Velu, C. Dupas, D. Renard, J. P. Renard, and J. Seiden, *Phys. Rev. B* **37**, 668 (1988).
- ¹⁷ P. Grünberg (private communication).
- ¹⁸ P. Etienne, J. Chazelas, G. Creuzet, A. Friederich, J. Massies, F. Nguyen Van Dau, and A. Fert, *J. Crystal Growth* **95**, 410 (1989); P. Etienne, S. Lequien, J. Massies, F. Nguyen van Dau, A. Fert, A. Barthelemy, G. Creuzet, and A. Friederich (these proceedings).
- ¹⁹ B. Dieny, J. P. Gavigan, and J. P. Rebouillat, in *Growth, Characterization and Properties of Ultrathin Magnetic Films and Multilayers*, edited by B. T. Jonker, J. P. Heremans, and E. E. Marinero, MRS Proceedings Vol. 151 (MRS, Pittsburgh, PA, 1989), p. 35.
- ²⁰ C. Kittel, *Introduction to Solid State Physics* 16th ed. (Wiley, New York, 1986), p. 426.
- ²¹ S. Lequien, C. Vettier, and M. Hennion (to be published).
- ²² In the presence of interface roughness the dipole interaction can give rise to an effective coupling between magnetic layers. However the "effective coupling field" arising from this mechanism cannot exceed a small fraction of $4\pi M_S$. This is much too low to account for the values of H_S found in Fe/Cr.
- ²³ L. L. Hinchey and D. L. Mills, *Phys. Rev. B* **33**, 3329, 1986.
- ²⁴ P. M. Levy, A. Fert, and S. Zhang (to be published).
- ²⁵ S. Maekawa and J. C. Slonczewski (private communication).
- ²⁶ We write \uparrow and \downarrow for the majority and minority spins, respectively.
- ²⁷ J. Friedel, *Recondizioni della Scuola "Enrico Fermi"* (Academic, New York, 1987).